Summary

We created three synthetic 'pseudoproxies' (Sr/Ca, $\delta^{18}O$, $\delta^{11}B$) with various amounts of environmental information encoded into each, based on their theoretical dependence on sea surface temperature (SST), sea surface salinity (SSS) and seawater pH (pH_{sw}). The means by which we calculated our three synthetic pseudoproxies are highly idealized, meaning that each pseudoproxy has a near-perfect relationship with its corresponding climate target(s). However, the uncertainty in each proxy ~ climate target relationship is considered in our experimental design, which examines how uncertainty in SST and pH estimates increases as the degree of Gaussian and autocorrelated noise increases. The magnitude of Gaussian noise and the degree of autocorrelation considered in our experiment is well beyond that which is typically observed in coral-based paleoclimate studies. We expect therefore that all sources of uncertainty, and their subsequent impacts on SST and pH estimates, are accounted for. The minimum uncertainty for each synthetic pseudoproxy was taken from the literature as analytical uncertainty. For synthetic Sr/Ca values, this was taken to be 0.009 mmol/mol, or approximately 0.1% RSD (Schrag, 1999). For synthetic $\delta^{18}O$ values, we used an analytical uncertainty of 0.1‰ (Epstein & Mayeda, 1953). For synthetic $\delta^{11}B$ values, analytical uncertainty was taken to be 0.18‰ (Stewart et al., 2021).

Environmental Data

Monthly SST and seawater pH data from the Great Barrier Reef (18.5ºS, 149.5ºE) between 1900 and 2000 were acquired from Lenton et al. (2016), a 20th century reconstruction of SST, SSS and pH_{sw} across the Great Barrier Reef (n = 1212). SSTs ranged from 21.83ºC to 29.69ºC (μ = 25.92ºC ± 1.91, 1σ), while pH_{sw} ranged from 8.09 to 8.21 (μ = 8.16 ± 0.03). Although SSS is also available from this dataset for the same time interval, the data are not reflective of realistic

salinity fluctuations in this region. Therefore, we used SSS data from the ORA20C dataset (de Boisséson et al., 2018) from the same location and time interval. SSS ranged from 31.61 to 34.17 practical salinity units (psu; μ = 33.69 ± 0.43 psu).

Synthetic Proxy Calculation

Synthetic Sr/Ca ratios were calculated as a function of SST using the mean slopes and intercepts for the Sr/Ca ~ SST relationship from (Corrège, 2006).

$$\frac{Sr}{Ca} = -0.0607(0.0090)T + 10.553(0.292) \quad (1)$$

Where *T* is temperature in degrees Celsius. Synthetic Sr/Ca ratios ranged from 8.75 to 9.23 mmol/mol (μ = 8.98 mmol/mol ± 0.12).

Synthetic $\delta^{18}O$ values were calculated as a function of both SST and SSS. First, the oxygen isotope ratio of seawater ($\delta^{18}O_{sw}$) was calculated as a function of SSS using the equation for the tropical Pacific from (LeGrande & Schmidt, 2006).

$$\delta^{18}O_{sw} = 0.27(0.006)SSS - 8.88(0.201) \quad (2)$$

Synthetic $\delta^{18}O$ values were then calculated by rearranging the temperature sensitivity equation from Epstein (1953) to a quadratic function.

$$T = 16.5 - 4.3(\delta^{18}O_c - \delta^{18}O_{sw}) + 0.14(\delta^{18}O_c - \delta^{18}O_{sw})^2 \quad (3)$$

Where $\delta^{18}O_c$ is the oxygen isotope ratio of carbonate. Finally, we subtracted 1.08 from the final synthetic $\delta^{18}O$ values, both to account for the correction factor to aragonite (+0.6) and to make

the values relative to VPDB (−1.68). Synthetic $\delta^{18}O$ values thus ranged from −4.58 to −2.47‰ (μ = −3.39‰ ± 0.48).

Synthetic $\delta^{11}B$ values were calculated as a function of SST, SSS and pH_{cf}. They were determined by rearranging the pH-dependent equation from (Zeebe & Wolf‐Gladrow, 2001) to solve for the boron isotope ratio of carbonate ($\delta^{11}B_c$).

$$pH = pK_b - \log\left(\frac{\delta^{11}B_{sw} - \delta^{11}B_c}{\delta^{11}B_c - \delta^{11}B_{sw} + 1000(\alpha - 1)}\right) \quad (4)$$

Where the boron isotope ratio of seawater ($\delta^{11}B_{sw}$) is 39.61‰ (Foster et al., 2010), and the mass fraction factor between boric acid and borate ion (α) is 1.0272 (Klochko et al., 2006). The negative log of the dissociation constant between boric acid and borate ion (*pKb*) is a function of both temperature and salinity. We therefore calculated *pKb* at each time interval by taking the negative log of the *Kb* equation from (Dickson, 1990). The values of *pKb* ranged between 8.56 and 8.64 given a temperature range between 21.83 and 29.69ºC and a salinity range between 31.61 and 34.17 psu.

These calculations yield synthetic $\delta^{11}B$ values between 18.30 and 19.64‰, which is expected given the pH of seawater. However, corals upregulate their internal pH relative to seawater (McCulloch et al., 2017) while also exhibiting greater seasonal variance (Ross et al., 2017). Thus, to yield synthetic $\delta^{11}B$ values consistent with those observed in coral aragonite, we calculated the pH of the calcifying fluid (pH_{cf}) from pH_{sw} using equation 14 from (D'Olivo et al., 2019).

$$pH_{cf} = 0.49pH_{sw} - 0.02T + 4.93 \quad (5)$$

Note that the temperature sensitivity of synthetic $\delta^{11}B$ values is realized in its dependence on both pKb as well as pH_{cf}. Meanwhile, the salinity sensitivity of synthetic $\delta^{11}B$ values is only realized in its dependence on pKb. Synthetic $\delta^{11}B$ values ranged from 22.21 – 24.10‰ (μ = 23.17‰ ± 0.41).

Error Assessments

We use three metrics to quantitatively compare SMITE SST and pH estimates with those derived from Sr/Ca ratios and $\delta^{11}B$ values, respectively: the correlation coefficient (*r*), the standard error of prediction (SEP), and the root-mean squared error (RMSE). Each metric provides a measure of the covariance, precision, and accuracy of the reconstruction, respectively. The SEP is calculated as the uncertainty in derived SST estimates based on the uncertainty in both the climate target (SST, pH_{sw}) as well as the uncertainty in the corresponding proxy / proxies. Given that our SST measurements are derived from, or modeled after, temperatures derived from *in situ* loggers, uncertainty for temperature was fixed at 0.02ºC (https://www.onsetcomp.com/products/data-loggers/u22-001). Uncertainty for our pH_{sw} measurements were fixed at a relatively conservative 0.02 units.

The SEP for each proxy ~ climate target relationship is calculated using a Monte Carlo approach. At each iteration (i = 1,…,10000), each individual measurement in both the proxy and climate target fields are randomly resampled from a normal distribution with a mean equal to the given proxy/climate target value (μ_i) and a standard deviation equal to the specified uncertainty (s_i). Model parameters are then estimated from the perturbed proxy and temperature fields, and SST/pH estimates for each data point are stored. The 95% confidence interval for each SST estimate is determined from the distribution of SST estimates derived from each Monte Carlo iteration. The SEP is then determined as the average distance from the mean to the upper and

lower bounds of the 95% confidence interval, divided by 1.96. The 95% confidence interval for the SEP itself is then defined as the standard deviation of the SEP throughout each calibration dataset, multiplied by 1.96.

Autocorrelated (Red) Noise

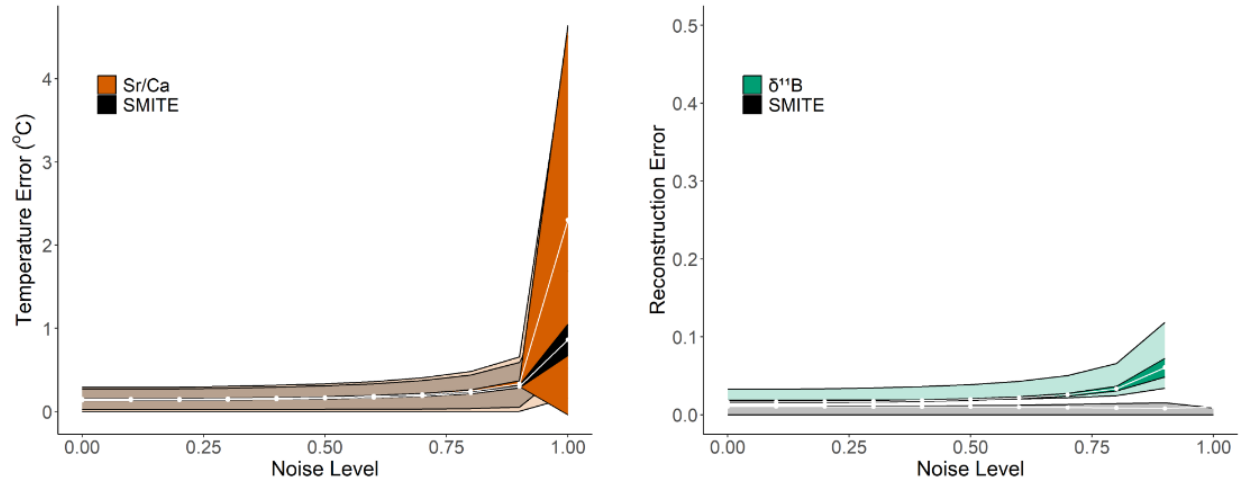

Figure 1. The precision (SEP; opaque envelope) and accuracy (RMSE; translucent envelope) of SMITE SST estimates (black) versus Sr/Ca-derived SST (left; orange) and $\delta^{11}B$-derived pH (right; green) over increasingly autocorrelated errors (fixed at analytical uncertainty).

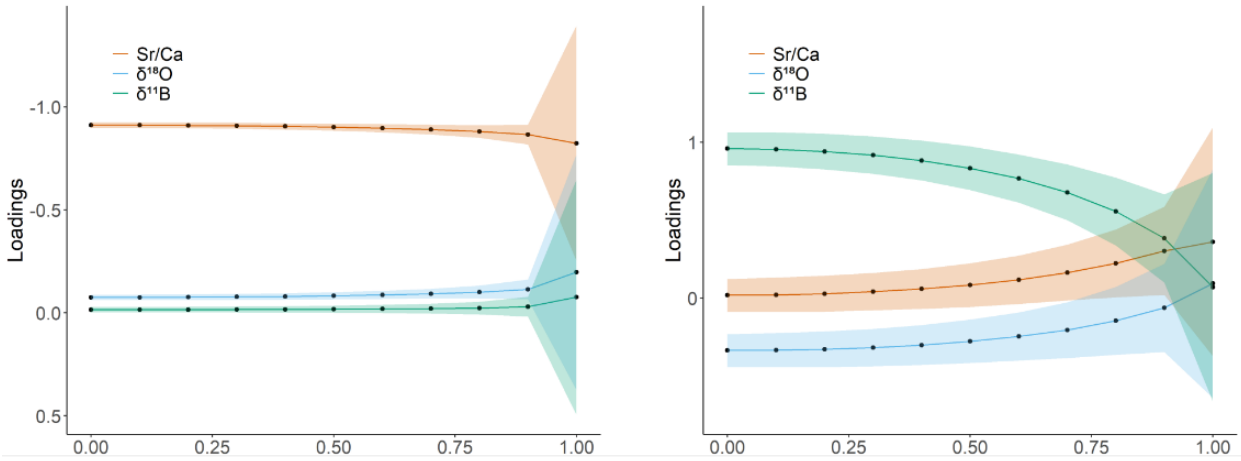

Figure 2. SMITE model parameters, or loadings, for SST (left) and pH (right) over increasingly autocorrelated errors (fixed at analytical uncertainty). Shaded regions represent the Monte Carlo estimated 95% confidence interval for each parameter (i = 10,000).

Calibration Period Length

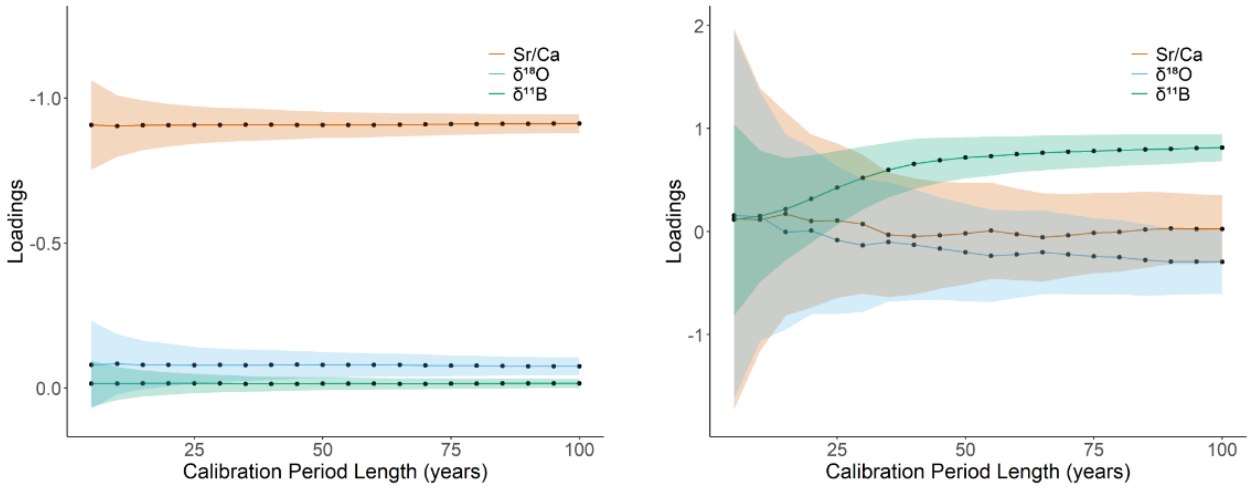

Figure 3. SMITE model parameters, or loadings, for SST (left) and pH (right) over different calibration period lengths. Shaded regions represent the Monte Carlo estimated 95% confidence interval for each parameter (i = 10,000).

References

Corrège, T. (2006). Sea surface temperature and salinity reconstruction from coral geochemical tracers. *Palaeogeogr. Palaeoclimatol. Palaeoecol.*, *232*, 408-428. https://doi.org/10.1016/j.palaeo.2005.10.014

D'Olivo, J. P., Ellwood, G., DeCarlo, T. M., & McCulloch, M. T. (2019). Deconvolving the long-term impacts of ocean acidification and warming on coral biomineralisation. *Earth Planet. Sc. Lett.*, *526*, 115785. https://doi.org/10.1016/j.epsl.2019.115785

de Boisséson, E., Balmaseda, M. A., & Mayer, M. (2018). Ocean heat content variability in an ensemble of twentieth century ocean reanalyses. *Clim. Dynam.*, *50*(9), 3783-3798. https://doi.org/10.1007/s00382-017-3845-0

Dickson, A. G. (1990). Thermodynamics of the dissociation of boric acid in synthetic seawater from 273.15 to 318.15 K. *Deep Sea Res. Part A*, *37*(5), 755-766. https://doi.org/10.1016/0198-0149(90)90004-F

Epstein, S., & Mayeda, T. (1953). Variation of O18 content of waters from natural sources. *Geochim. Cosmochim. Acta*, *4*(5), 213-224. https://doi.org/10.1016/0016-7037(53)90051-9

Foster, G. L., Pogge von Strandmann, P. A. E., & Rae, J. W. B. (2010). Boron and magnesium isotopic composition of seawater. *Geochem. Geophys. Geosyst.*, *11*. https://doi.org/10.1029/2010GC003201

Klochko, K., Kaufman, A. J., Yao, W., Byrne, R. H., & Tossell, J. A. (2006). Experimental measurement of boron isotope fractionation in seawater. *Earth Planet. Sc. Lett.*, *248*, 276-285. https://doi.org/10.1016/j.epsl.2006.05.034

LeGrande, A. N., & Schmidt, G. A. (2006). Global gridded data set of the oxygen isotopic composition in seawater. *Geophys. Res. Lett.*, *33*(12). https://doi.org/10.1029/2006GL026011

McCulloch, M. T., D'Olivo, J. P., Falter, J., Holcomb, M., & Trotter, J. A. (2017). Coral calcification in a changing World and the interactive dynamics of pH and DIC upregulation. *Nat. Commun.*, *8*, 15686. https://doi.org/10.1038/ncomms15686

Ross, C. L., Falter, J. L., & McCulloch, M. T. (2017). Active modulation of the calcifying fluid carbonate chemistry (δ 11 B, B/Ca) and seasonally invariant coral calcification at sub-tropical limits. *Sci. Rep.*, *7*, 1-11. https://doi.org/10.1038/s41598-017-14066-9

Schrag, D. P. (1999). Rapid analysis of high‐precision Sr/Ca ratios in corals and other marine carbonates. *Paleoceanography*, *14*, 97-102. https://doi.org/10.1029/1998PA900025

Stewart, J. A., Christopher, S. J., Kucklick, J. R., Bordier, L., Chalk, T. B., Dapoigny, A., Douville, E., Foster, G. L., Gray, W. R., Greenop, R., Gutjahr, M., Hemsing, F., Henehan, M. J., Holdship, P., Hsieh, Y.-T., Kolevica, A., Lin, Y.-P., Mawbey, E. M., Rae, J. W. B., . . . Day, R. D. (2021). NIST RM 8301 Boron Isotopes in Marine Carbonate (Simulated Coral and Foraminifera Solutions): Inter-laboratory δ11B and Trace Element Ratio Value Assignment. *Geostand. Geoanal. Res.*, *45*(1), 77-96. https://doi.org/10.1111/ggr.12363

Zeebe, R. E., & Wolf‐Gladrow, D. A. (2001). *CO2 in Seawater: Equilibrium, Kinetics, Isotopes*.